行政院國家科學委員會專題研究計畫　成果報告

操作奈米粒子之動力學分析與控制(II)

計畫類別：個別型計畫
計畫編號：NSC92-2212-E-009-031-
執行期間：92 年 08 月 01 日至 93 年 07 月 31 日
執行單位：國立交通大學機械工程研究所

計畫主持人：呂宗熙

報告類型：精簡報告
報告附件：出席國際會議研究心得報告及發表論文
處理方式：本計畫可公開查詢

中　華　民　國 93 年 10 月 28 日

操作奈米粒子之動力學分析與控制(II)

(計劃編號 NSC92-2212-E-009-031，執行期限 2003.08.01 ~ 2004.07.31)

呂 宗 熙

新竹市 國立交通大學 機械工程研究所

***Abstract*—To develop nanotechnology, nanoparticle manipulation plays an important role in the assembly of nanoelements. To overcome the physical and chemical phenomenon at nano scale during pushing nanoparticles, strain gauges are sensed to actuate an X-Y stage in an atomic force microscopy (AFM) system to push nanoparticles based on vector lithography. The results of manipulation demonstrate pushing nanoparticles at the inclination of substrate, the limited scanning range in the different inclination, and removing and remaining the nanoparticles at the inclination of substrate. In addition, a fuzzy controller is responsible for compensating "tip-particle contact loss" by signals of a laser-detector system, so as to establish an accurate and stable manipulation system.**

***Index terms*—Nanoparticle, X-Y stage, AFM.**

1 INTRODUCTION

IMAGING of any type of micrometer- and nanometer-sized objects in any type of environment down to atomic and molecular resolution has become possible by the invention of the AFM. An AFM probe has been recently utilized as a simple nanomanipulator for pushing based positioning of nanometer-sized objects, cutting, nanolithography applications, etc.

In this study, an X-Y stage in an AFM is actuated to manipulate nanoparticles of 50 nm radius in three–dimension (3-D) based on investigation results in 1-D and 2-D. In order to make 3-D movement of nanoparticles, the height between the substrate and X-Y stage has to be adjusted. Moreover, the difference between pushing up and pushing down will be observed, and which way is easier to push will be discussed. Finally, experimental results demonstrate pushing nanoparticles on an inclined substrate, the limitation of scanning range in the different inclination, and removed and remained nanoparticles on the inclined substrate.

1.1 Literature Survey

Nano-manipulation using atomic force microscopy (AFM) has attracted much attention among researchers. Sitti and Hashimoto [2000] presented that the latex particles with 242- and 484-nm radii can be positioned on a Si substrate successfully at around 30-nm accuracy. In another work of Sitti [2004], 500-nm radius gold-coated latex particles are pushed on a silicon substrate. Frictional parameters and behavior are estimated using the proposed models and experimental pushing force data.

Hsieh et al. [2002] have deposited gold nanorods on a Si substrate, obtained the rod images using dynamic mode in AFM, and subsequently performed manipulation using the AFM tip. Akai et al. [2001] manipulated insulated molecular wires with the cantilever tip of an AFM and found that the insulated molecular wire was moved or cut off by the manipulation process. The manipulation results with varying AFM tip loading forces indicated that the insulated molecular wire is cut off at loading forces larger than approximately 30 nN.

It is well known that the main difficulty of nanomanipulation using AFM is the lack of real-time visual feedback. Hence, Li et al. [2004] developed augmented reality system has solved this problem by locally updating the AFM image in real-time based on measured force information during nanomanipulation. The real-time visual display combined with the real-time force feedback provides an augmented reality environment, in which the operator not only can feel the interaction forces but also can observe the real-time changes of the nano environment.

The AFM is a powerful tool for imaging biological molecules on a substrate. However, there is no effective time axis with AFM; AFMs require minutes to capture an image, but many biological processes occur at a much higher rate. Hence, Ando et al. [2002] sought to increase markedly the scan speed of the AFM, and developed various devices optimized for high-speed scanning. Combining these devices has produced an AFM that can capture a 100 × 100 pixel image within 80 ms, thus generating a movie consisting of many successive images of a sample.

Recently, He et al. [2002] has adopted an electrophoresis method, which is usually used in biosciences, to mount single nanowires onto chosen electrodes of a prototype device. Fu et al. [2004] have reported a microchip device that uses traveling-wave-dielectrophoretic forces to manipulate microparticles and yeast cells. Furthermore, nanostructures are constructed nano building blocks based on multiwalled carbon nanotubes through 3-D nanorobotic manipulation [Dong et al., 2004].

1.2 Objective

To achieve higher accuracy of position nanoparticles in 3-D, this study utilizes an X-Y stage which has higher precision in an AFM system to scan sample profile and to position nanoparticles. Fuzzy control will be utilized to compensate tip-particle contact loss by signals of a laser-detector system, so as to establish an accurate and stable manipulation system.

2. MANIPULATION STRATEGY

In this study, golden nanoparticles on a Si substrate are to be pushed using a Si fabricated AFM cantilever tip in ambient conditions. At first, the image of nanoparticle is obtained using AFM semicontact-mode imaging, and then using contact-mode may move the nanoparticles. Assuming the particle is pushed along the y-axis or x-axis, this study deals with two-dimensional (2-D) pushing strategy. A constant height control strategy is utilized. Motion steps that realize AFM-based pushing in y-axis or x-axis are shown in Fig. 2.1, where F denotes the farther final position of the particle in pushing down.

1. <1→2>: The tip is moved along the z direction until detecting the contact with the substrate by measuring

the cantilever deflection (absolute tip-substrate distance is not known initially).

2. <2 → 3>: The substrate is moved along the desire direction until detecting the contact between the tip and the particle by cantilever deflection detection, and then stopped.
3. <3→5>: The particle is just pushed for a maximum distance $\Delta d_{\max}$ by moving the substrate due to the inclination of the substrate.

In Step 3, the tip and particle may lose contact due to positioning errors, and particle rotation/spinning along the z-axis during pushing. Once it occurs, y-axis or x-axis motion should stop, and the tip must return to the position where contact begins by two axes controllers. Step 3 in the pushing scheme is repeated until there is no contact loss.

The tip is not raised or lowered during pushing in AFM contact mode. That is, when substrate tilts, the tip is kept horizontal during pushing. Accordingly, the tip and particle in pushing down would lose contact inevitably. Therefore, there is the maximum distance in pushing the gold nanoparticle down the inclined substrate, as shown in Fig 2.2. The maximum distance is written as

$$\Delta d_{ta} + \Delta d_{\max} \cong \frac{2R_a}{\tan\theta} \quad (2.1)$$

where Δd_{ta} is the original distance between AFM tip and particle, $\Delta d_{\max}$ is the maximum distance of the particle pushing, R_a is the particle radius, and θ is the inclination of the substrate.

According to this pushing strategy, pushing up can succeed easier than pushing down obviously. Certainly, Eq. (2.1) ignores the nanoparticle sprung by AFM probe tip and rolling itself. Moreover, assuming the particle is purely sliding and the substrate is smooth enough.

In order to create the inclination angle at 1°, 2°, and 3°, we have to pad the substrate high , for example, $\tan 1^\circ \cong 0.0175$, $\tan 2^\circ \cong 0.0349$, and $\tan 3^\circ \cong 0.0524$. As a consequence, when the width of the bottom is 10000 nm, the heights become 175 nm, 349 nm, and 524 nm, respectively. If $\theta = 0.1^\circ \sim 3^\circ$ and $R_a = 50$ nm, substituting these parameters are substituted into Eq (2.1) and plotted as depicted in Fig. 2.3. In order to make the inclination of the substrate, it will be illustrated in chapter 5.

3. FUZZY CONTROL

In Fig. 3.1, in addition to tip-particle contact loss or other operating errors during pushing of nanoparticles also influences plant performance. Therefore, these error sources will be analyzed and compensated by fuzzy controller in this study.

In this study, tip-particle contact loss and static friction sticking will be taken into account for the operating errors. Tip-particle contact loss is that:

During pushing, tip-particle contact can be lost due to the rotation/spinning of a particle along the z-axis, and the x-y positioning errors.

Static friction sticking is that:

A particle sticks to a substrate during initial pushing due to static friction.

In this study, the nanoparticle is assumed to be pushed along the y-axis or x-axis; otherwise stay at its position if contact loss occurs. From measured lateral force signals of the cantilever, as shown in Fig. 3.2, x-y positioning errors can be predicted as (e_x, e_y) for precise positioning, where the signals of Fig. 3.2 are positive during the tip slides toward right side of the nanoparticle, and that are negative during the tip slides toward left side, whereas if that are zero, the tip does not slide towards any sides. Therefore, fuzzy controller will be utilized to compensate the errors by the signals of Fig. 3.2, as shown in Fig. 3.1. Since the x-axis and y-axis plants are designed independently, fuzzy controller will compensate x-axis and y-axis positions, respectively. In order to restrain two-error sources, static friction-sticking error is first compensated. During initial pushing, the particle sticks to the substrate to cause an offset value (x_{sf}, y_{sf}) that should be compensated. These offset values are observed directly from experimental data. Subsequent to static friction sticking, compensated tip-particle contact loss error is the second step. From Fig. 3.2, after detecting tip-particle contact loss (L point) at (x_l, y_l), the x-y motion is stopped to set compensated error values as $(\varepsilon_x, \varepsilon_y) = (x_l - x_n, y_l - y_n)$, where x_n and y_n are the tip position after the contact loss. In this study, fuzzy control will be utilized for the compensations and illustrated in the next section.

4. SIMULATION RESULTS

In this study, in order to compensate tip-particle contact loss error during pushing nanoparticle, a fuzzy compensated controller is utilized. Static friction sticking error will be compensated form experimental data by pre-compensator. Since the fuzzy controller will be utilized to compensate tip-particle contact loss error, an input signal of the fuzzy controller is lateral-force signal, while output signals are x-axis and y-axis compensated displacements, which are related by a circle of radius R=50nm. According to this one-input-two-output model of the fuzzy controller and some system's features, a fuzzy rule base can be constructed as shown in Table 4.1, where NB is negative big, NM is negative medium, NS is negative small, ZE is zero, PS is positive small, PM is positive medium, and PB is positive big fuzzy set.

Assuming command input starts to send at 0.01 sec and tip-particle contact loss occurs at 0.0102, 0.0112, 0.0124, and 0.0138 sec. When tip-particle contact loss occurs, the fuzzy controller will compensate y-axis position first and then compensate x-axis. Simulated results of fuzzy control by using the MATLAB and Simulink softwares are shown in Fig. 4.

5. EXPERIMENTAL RESULT

5.1 Preparation of Gold Nanoparticles

In this study, since gold nanoparticles of the average radius $R_a = 50$ nm are to be manipulated, the preparation of gold nanoparticles will be discussed first. The preparation steps of gold nanoparticles are:

1. Dilute gold colloids of BBI Co. (EM. GC 100) with

water by at least tenfold.
2. Drop one diluted gold colloid on silicon substrate.
3. Bake the gold colloid on silicon substrate in a vacuum oven for 2hr at 60°C.

By employing the above-mentioned steps, the scanning image by using an AFM is obtained as shown in Fig. 5.1.

5.2 Manipulation of Gold Nanoparticles

According to the profile in Fig. 5.2, the inclination of the substrate is $a\tan(40/10000) \cong 0.23^\circ$ in x-direction and the gold nanoparticle is about 100 nm height.

As shown in Fig 5.3 and in Fig 5.4, it is taken three times to achieve the target I in pushing the gold nanoparticle by the vector lithography up the inclination of the substrate, but six times in pushing down. Therefore, it demonstrated pushing up is easier than pushing down.

In this experiment, the angle of the inclination θ is 0.23°, and the diameter $2R_a$ of nanoparticle is 100 nm. Substituting parameters into Eq. (2.1) would yield $\Delta d_{ta} + \Delta d_{\max}$ about 24911 nm in pushing down.

Figs. 5.5, 5.6, and 5.7, where padding one, two, and three pieces of paper of thickness 0.6 mm in y-direction makes the inclination angle at the average 0.85°, 1.59°, and 2.12° in Table 5.1, respectively. Although adding paper can raise the inclination angle, the range of height is limited to 1600 nm due to AFM. That is, beyond the height of 1600 nm and below the height of 0 nm can not obtain topography.

Due to the height limitation, the scanning range in y-direction is also limited, respectively. As shown in Figs. 5.8, 5.9, and 5.10, the scanning range in y-direction is limited to $1700 \times (\tan 0.85^\circ)^{-1} \cong 114583$, $1700 \times (\tan 1.59^\circ)^{-1} \cong 61244$, and $1500 \times (\tan 2.12^\circ)^{-1} \cong 40521$, respectively. Accordingly, the more inclined it is, the less the scanning range is obtained.

Examples on a Ni sample surface are shown in Fig. 5.11, which displays a series of AFM pictures where gold nanoparticles were removed limited only by the size of the scan range. All images in Fig. 5.11 were obtained using the tapping mode and nanoparticles were pashed in the contact mode. Fig. 5.11 shows the nanoparticles on the borderland deposited forming the Dipper and also shows that the substrate higher in the right side and lower in the left side. As depicted in Figs. 5.11(a) to (e), the red ovals represent the nanoparticles pushed away afterwards. In Fig. 5.11(f) the white arrow shows a nanoparticle subject to unexpected pushing and is to be pushed back to the original position. In Fig. 5.11(g) the new position of the nanoparticles is indicated. Fig 5.12 shows the 3-D topography of Fig. 5.11(g). Fig. 5.13 shows the height of the white line in Fig.5.12.

6. CONCLUSION

This study uses fuzzy control to compensate displacement error in manipulating nanoparticles. To demonstrate the proposed method, simulation and experimental results have been carried out. According to the results, this study concludes the following:

1. The maximum distance in pushing the gold nanoparticle down an inclined substrate has been established.
2. A fuzzy controller for compensating static friction sticking and tip-particle contact loss has been designed.
3. According to experimental results in Figs. 5.3 and 5.4, pushing nanoparticle up the inclined substrate is easier than pushing down.
4. From experimental results in Figs. 5.5 to 5.10, adding paper can raise the inclination angle, the range of height is limited to 1600 nm due to AFM, and the scanning range in y-direction is also limited.
5. In relation to experimental results in Figs. 5.11, 5.12, and 5.13 demonstrated the performance of position control for nanoparticles removed and remaining on an inclined substrate.

REFERENCES

Akai, T., Abe, T., Shimomura, T., and Ito, K., "Manipulation of Insulated Molecular Wire with Atomic Force Microscope", Jpn. J. Appl. Phys., Vol. 40, No. 12A, pp. L1327-L1329, December 2001

Ando, T., Kodera, N., Maruyama, D., Takai, E., Saito, K., and Toda, A., "A High-Speed Atomic Force Microscope for Studying Biological Macromolecules in Action", Jpn. J. Appl. Phys., Vol. 41, No. 7B, pp. 4851-4856, July 2002

Dong, L., Arai, F., and Fukuda, T., "Destructive Constructions of Nanostructures With Carbon Nanotubes Through Nanorobotic Manipulation", IEEE/ASME Trans. on Mechatronics, Vol. 9, No. 2, June 2004.

Dorf, R.C., and Bishop, R.H., Modern Control Systems, Prentice-Hall, Inc., New Jersey, 9th ed., 2001.

Fu, L.M., Lee, G.B., Lin, Y.H., and Yang, R.J., "Manipulation of Microparticles Using New Modes of Traveling-Wave-Dielectrophoretic Forces: Numerical Simulation", IEEE/ASME Trans. on Mechatronics, Vol. 9, No. 2, June 2004.

He, J. Z., Xu, J. B., Xu, M. S., Xie, Z., and Wilson, I. H., "Dispersion, Refinement, and Manipulation of Single Silicon Nanowires," Vol. 80, No. 10, pp. 1812-1816, 2002.

Hsieh, S. Meltzer, S., Wang, C. R. Chris, Requicha, A. G., Thompson, M. E., and Koel, B. E., "Imaging and Manipulation of Gold Nonorods with an Atomic Force Microscope," Vol. 106, No. 2, pp. 231-234, January 2002.

Li, G.., Xi, N., Yu, M., and Fung, W.K., "Development of Augmented Reality System for AFM-Based Nanomanipulation", IEEE/ASME Trans. on Mechatronics, Vol. 9, No. 2, June 2004.

Sitti, M. and Hashimoto, H., "Controlled Pushing of Nanoparticles: Modeling and Experiments", IEEE/ASME Trans. on Mechatronics, Vol. 5, No. 2, June 2000.

Sitti, M., "Atomic Force Microscope Probe Based Contorlled Pushing for Nanotribological Characterization", IEEE/ASME Trans. on Mechatronics, Vol. 9, No. 2, June 2004.

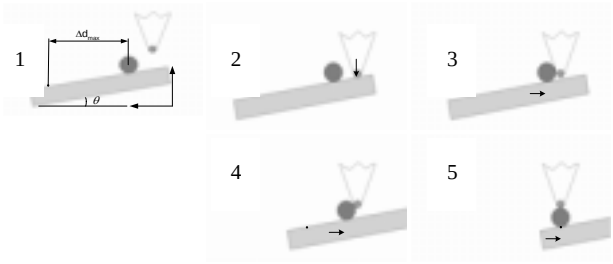

Fig. 2.1 AFM-based automatic 2-D particle pushing strategy

AFM ti

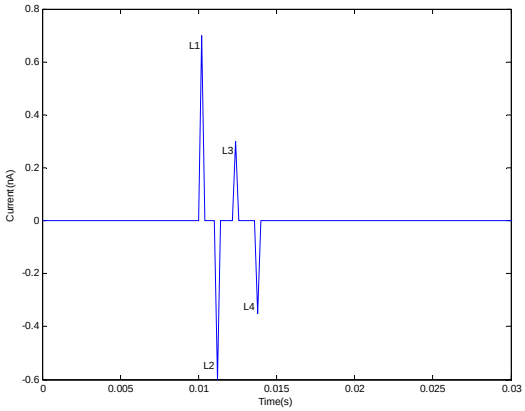

Fig. 3.2 Assumed Lateral-Force Signal of the Cantilever

nanoparticle P

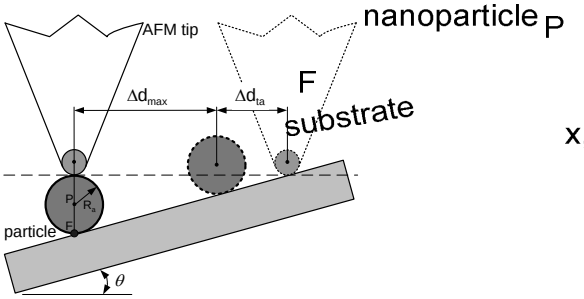

Fig. 2.2 The Maximum Distance in Pushing the Gold Nanoparticle down the Inclination of the Substrate

x, y plan

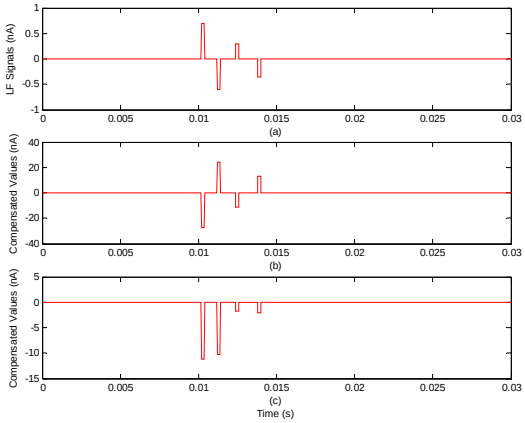

Fig. 4 Simulation Results of Fuzzy Controller
(a) LF Signals (b) X-Axis (c) Y-Axis Compensated Values

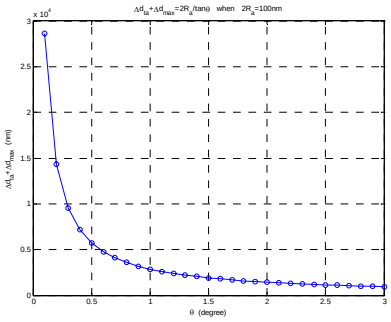

Fig 2.3 The Relation between the Maximum Distance in Pushing the Gold Nanoparticle down and the Inclination of the Substrate in $\theta = 0.1^\circ \sim 3^\circ$

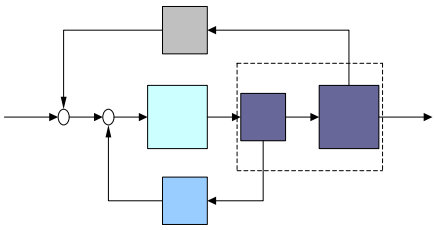

Fig. 3.1 Whole Pushing Control System Diagram

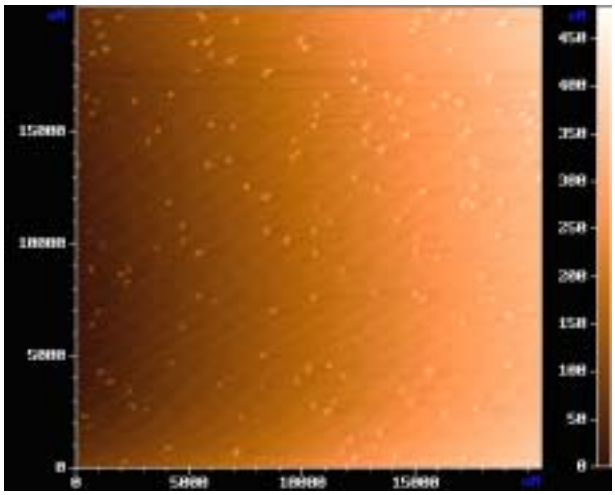

Fig. 5.1 Scanning Image of 100nm Nanoparticle

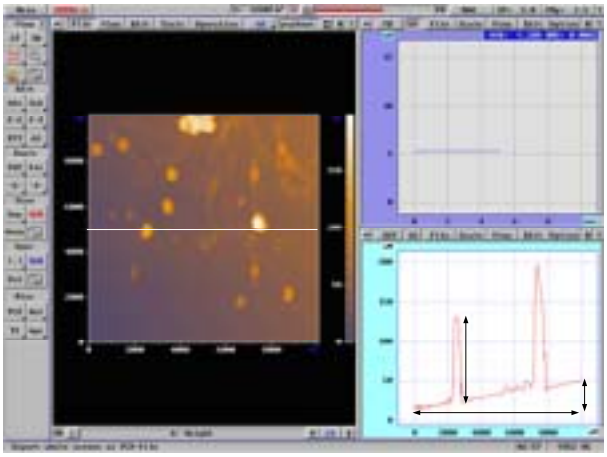

Fig. 5.2 Inclination of Substrate and Height of Gold Nanoparticle

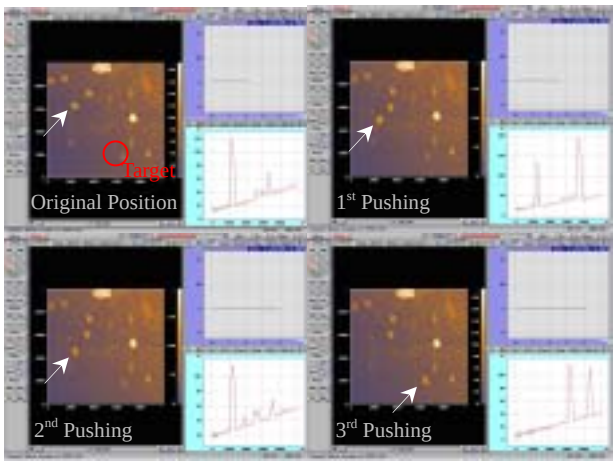

Fig. 5.3 Three Times of Pushing up Process and Corresponding X-Direction Profile

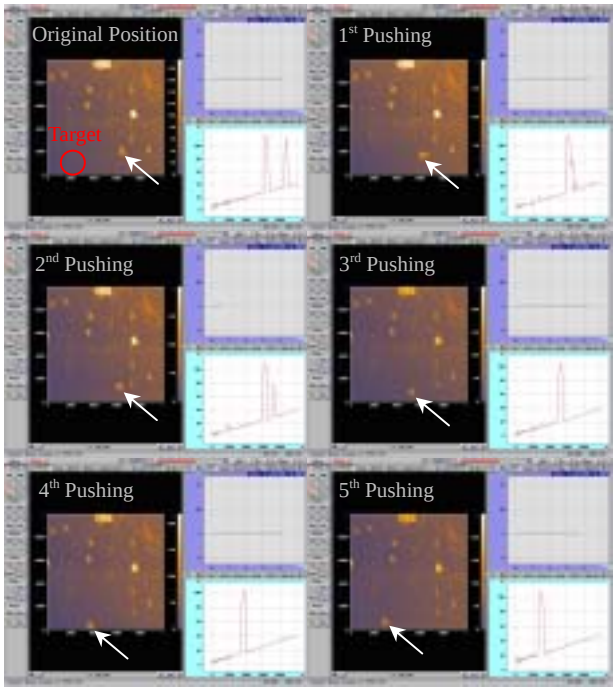

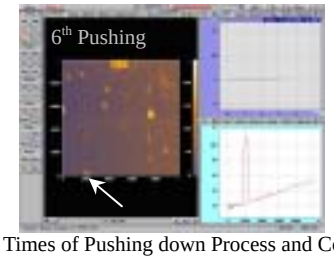

Fig. 5.4 Six Times of Pushing down Process and Corresponding X-Direction Profile

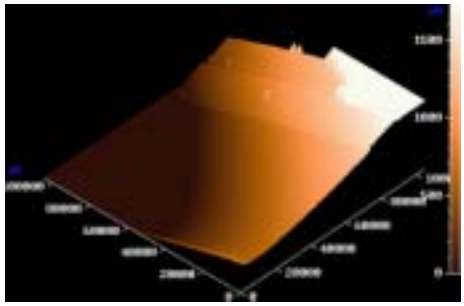

Fig. 5.5 3-D Topography of Padding One Piece of Paper

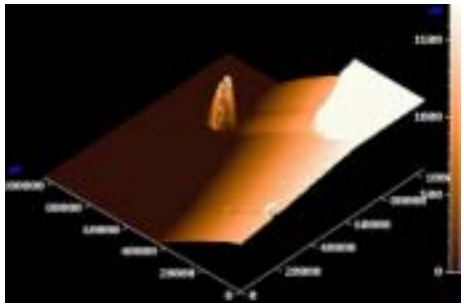

Fig. 5.6 3-D Topography of Padding Two Piece of Paper

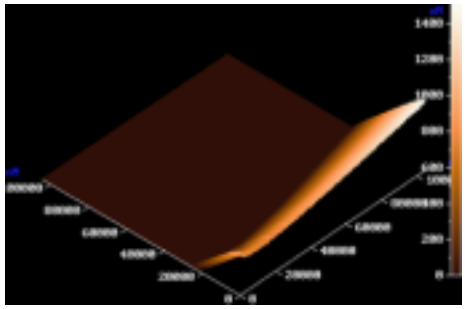

Fig. 5.7 3-D Topography of Padding Three Piece of Paper

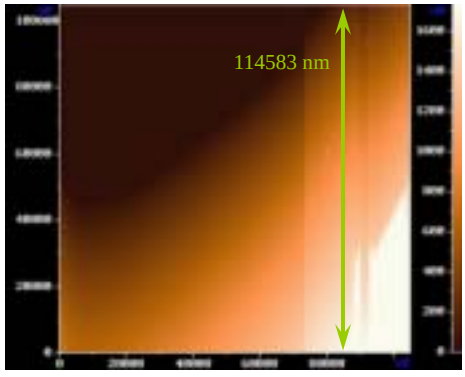

Fig. 5.8 Limited scanning range of 114583nm at inclination angle 0.85°

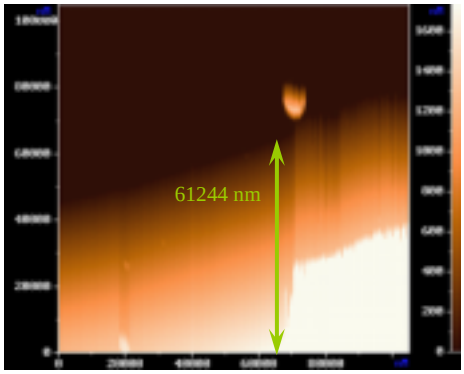

Fig. 5.9 Limited scanning range of 61244nm at inclination angle 1.59°

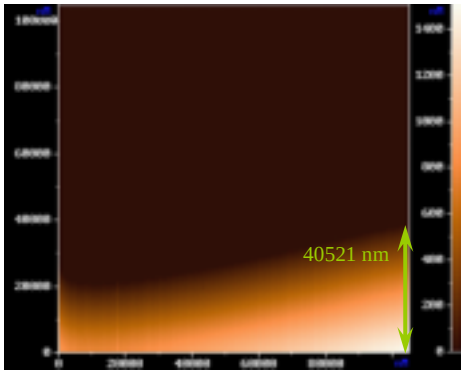

Fig. 5.10 Limited scanning range of 40521nm at inclination angle 2.12°

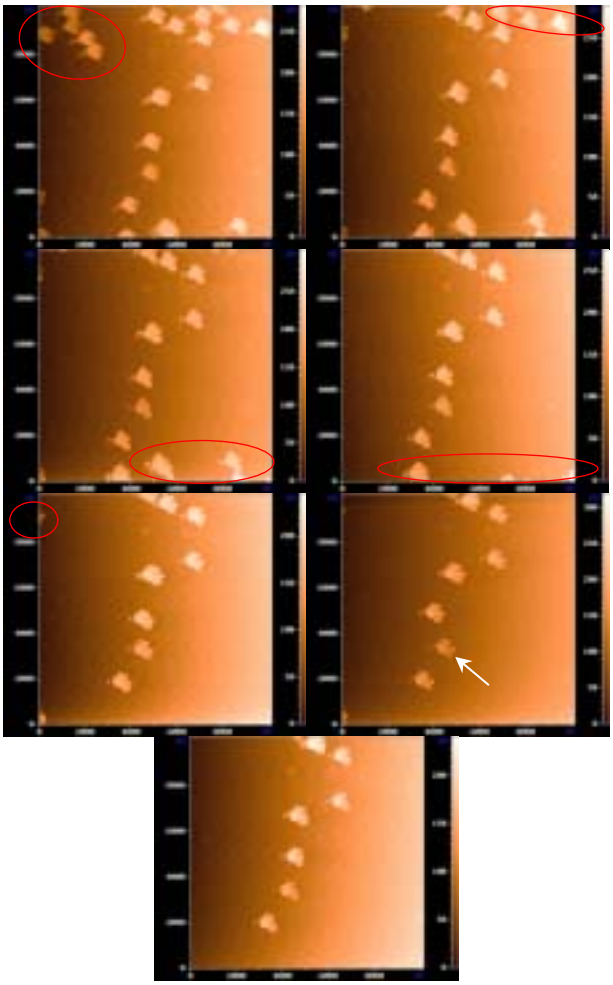

Fig. 5.11 Removing Minor Nanoparticles and Remaining Main Ones

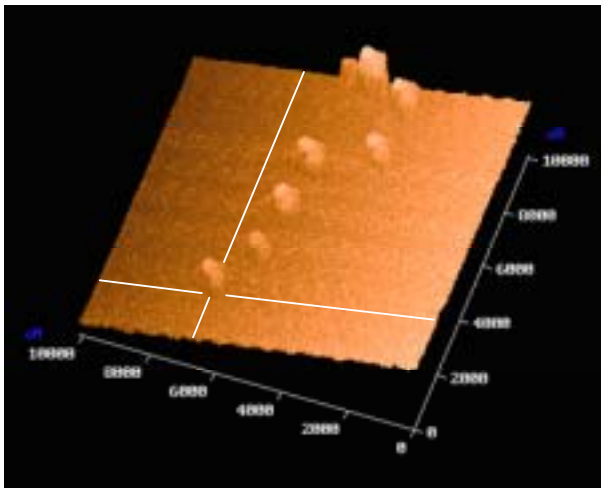

Fig. 5.12 3-D Topography of Fig. 5.10 (g)

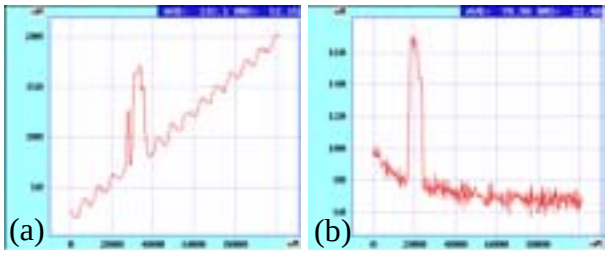

Fig. 5.13 Height of Fig. 5.11 (a) X-Coordinate (b) Y-Coordinate

Table 3.1 Fuzzy Rulebase

Output / Input	X-Axis Compensated Values	Y-Axis Compensated Values
NB	PB	B
NM	PM	M
NS	PS	S
ZE	ZE	ZE
PS	NS	S
PM	NM	M
PB	NB	B

Table 5.1 Angle of Inclination

	X coordinate				
No. of paper	at 0 nm	at 30000 nm	at 60000 nm	at 90000 nm	Average
1 paper	0.82	0.81	0.85	0.91	0.8475
2 papers	1.54	1.55	1.54	1.74	1.5925
3 papers	2.02	2.1	2.17	2.19	2.12

(unit: degree)